Vol. 750: 133–152, 2024
https://doi.org/10.3354/meps14728

MARINE ECOLOGY PROGRESS SERIES
Mar Ecol Prog Ser

Published December 5

Connectivity of scamp *Mycteroperca phenax* populations in the United States Gulf of Mexico and Atlantic Ocean

J. Roger Brothers[1,*], Kyle W. Shertzer[2], Mandy Karnauskas[3], Ana C. Vaz[3,4], Nathan M. Bacheler[2], Claire B. Paris[5]

[1]University of Maine, School of Marine Sciences 350 Commercial Street, Portland, ME 04101, USA
[2]National Oceanic and Atmospheric Administration, Southeast Fisheries Science Center, 101 Pivers Island Road, Beaufort, NC 28516, USA
[3]National Oceanic and Atmospheric Administration, Southeast Fisheries Science Center, 75 Virginia Beach Drive, Miami, FL 33149, USA
[4]Cooperative Institute For Marine and Atmospheric Studies, University of Miami, 4600 Rickenbacker Causeway, Miami, FL 33149, USA
[5]University of Miami, Rosenstiel School of Marine, Atmospheric, and Earth Science, 4600 Rickenbacker Causeway, Miami, FL 33149, USA

ABSTRACT: Connectivity among marine fish populations not only arises through the movement of adults but also through larval dispersal facilitated by ocean currents. For species with long pelagic larval duration and high site fidelity as adults, larval dispersal can be the dominant mechanism of connectivity among otherwise spatially distinct populations. Therefore, when assessing the recruitment dynamics or population structure of such species, it is essential to evaluate how larval biology and reproductive ecology interact with oceanographic circulation. To investigate this interaction for scamp *Mycteroperca phenax*, a grouper found in the Gulf of Mexico and Atlantic Ocean, we simulated the dispersal of millions of virtual larvae throughout the scamp's range near the southeastern USA. We found a pattern of local retention, with larvae tending to settle close to their spawning location. There was also, however, long-distance dispersal that consistently crossed the boundary between spatial management units. Due to directional patterns in oceanographic transport and spatial differences in abundance, almost one-third of the virtual larvae that settled in the Atlantic came from spawning locations in the Gulf of Mexico, although most of these settled near the boundary between the regions. These patterns were robust to a variety of sensitivity analyses, but the magnitude of connectivity between management units varied. This connectivity has significant implications for stock assessment and fishery management. It may increase the resilience of Atlantic populations, but it also means that the sustainability of Atlantic populations may rely, in part, on the health of spawning populations in the Gulf of Mexico.

KEY WORDS: Connectivity · Larval dispersal · Grouper · Reef fish · Stock structure · Fisheries management

1. INTRODUCTION

Movement patterns and site fidelity strongly influence the population connectivity and spatial structure of genetic differentiation in a species. Connectivity requires movement, so species with high movement rates or distances are commonly associated with a high degree of mixing and more homogeneous genetic structure on broad spatial scales (Palumbi 2003, Young et al. 2015, Carr et al. 2017). Species with strong site fidelity, however, are typically characterized by population structures with strong spatial patterns of genetic differentiation (Meylan et al. 1990, Campbell et al. 2008, Rooker et al. 2008, Bonanomi et al. 2016). This is often due to natal site fidelity, whereby an animal either remains at its natal location (philopatry) or re-

*Corresponding author: jroger.brothers@gmail.com

turns to reproduce at its natal location after an initial migration away (natal homing). However, spatial population structure can also arise through foraging site fidelity to non-natal locations by juveniles or adults (Lowther et al. 2012).

Sometimes, however, diverse taxa, ranging from birds (Milot et al. 2008, Pearce et al. 2008) to fishes with varied life histories, exhibit little genetic differentiation across broad spatial scales despite natal homing (Thorrold et al. 2001), site fidelity (Whitney et al. 2012, Klein et al. 2022), or the sedentary behavior of adults (van Herwerden et al. 2009, Berry et al. 2012, Gardner et al. 2015, Antoni & Saillant 2017). This can lead to a perceived mismatch in the scale of demographic connectivity, which considers the exchange of individuals between populations, and estimates of geneflow (Weersing & Toonen 2009, Lowe & Allendorf 2010, Selkoe et al. 2016, Legrand et al. 2022). Such is the case for scamp *Mycteroperca phenax*, an economically important reef-associated grouper that is found throughout the continental shelf off the southeastern USA — from the northwest Gulf of Mexico to the Atlantic Ocean near North Carolina (Smith 1971, Bullock & Smith 1991, Bacheler & Ballenger 2018).

Scamp form spawning aggregations (<100 individuals) in high-relief rocky areas along the edge of the continental shelf (Coleman et al. 2011, SAFMC 2013, Farmer et al. 2017, Grüss et al. 2018, Heyman et al. 2019) that are thought to comprise both resident and transient individuals (Biggs et al. 2021). The details are not well established, but compared to other aggregating groupers, like gag *Mycteroperca microlepis*, scamp aggregations are thought to be less specific to particular locations or habitat types (Coleman et al. 2011). Some localized movement to and from spawning locations on the edge of the continental shelf is likely, but there is no direct evidence of significant migration. Tag recaptures overwhelmingly find scamp within 20 km of their release location, with only a handful of documented individuals traveling farther (Wilson & Burns 1996, Coleman et al. 2011, Addis et al. 2013, SEDAR 2020).

Nonetheless, genetic analyses of scamp have found no spatial patterns of differentiation or population structure. Instead, a single genetic population spans the continental shelf off the southeast USA, including the Gulf and Atlantic regions (Zatcoff et al. 2004, SEDAR 2020). This finding has led to speculation about the mechanism of mixing that maintains genetic homogeneity across the scamp population, despite high site fidelity and little post-settlement movement.

One plausible explanation is that long-distance larval dispersal by ocean currents facilitates connectivity between disparate and otherwise isolated populations (Zatcoff et al. 2004). Indeed, larval dispersal has long been implicated as a source of population connectivity in fishes (Cowen et al. 2003). For taxa with long pelagic larval durations (PLDs), such as grouper (Lindeman et al. 2000), it may serve as the dominant form of connectivity. The dispersal distances required to mix scamp populations in the Gulf of Mexico with those in the Atlantic, however, are orders of magnitude greater than what is commonly assumed to be realized (Cowen et al. 2006, Abesamis et al. 2017, Almany et al. 2017, D'Aloia et al. 2022). Moreover, the dispersal patterns of reef-fish larvae, including grouper species, are widely thought to be dominated by self-recruitment, with most larvae settling close to where they spawned (Jones et al. 1999, 2005, Cowen et al. 2006, Buston et al. 2012, Almany et al. 2013, D'Aloia et al. 2015).

In US waters, scamp are managed as 2 separate stocks: one in the Gulf of Mexico, which is managed by the Gulf of Mexico Fishery Management Council and was recently estimated to be not overfished and not subject to overfishing (SEDAR 2022a); another in the Atlantic, which is managed by the South Atlantic Fishery Management Council and was recently estimated to be overfished but not subject to overfishing (SEDAR 2022b). This 2-stock structure is due, in part, to geographical boundaries as well as a presumed biological separation between populations. In effect, this treats US scamp in the Gulf of Mexico and Atlantic as 2 independent and homogeneous populations. If, however, sufficient larval dispersal exists to mix scamp populations in the 2 regions, then it could also have implications for fishery management.

In particular, spatial management decisions, like the placement of stock boundaries and marine protected areas, benefit from understanding which areas provide recruitment to the broader region and which areas rely on external recruitment (Dubois et al. 2016). These so-called 'source–sink' dynamics can be quantified by simultaneously considering a variety of connectivity metrics, including some that consider the retention of locally spawned larvae and others that consider the exchange of larvae between areas (Dubois et al. 2016). Moreover, understanding dispersal could influence the way recruitment is modeled during stock assessment. For example, in some instances, statistical models that include connectivity metrics better predict inter-annual recruitment deviations than conventional spawner–recruit relationships do (Hidalgo et al. 2019).

Therefore, to investigate the scale of scamp connectivity, we used an individual-based model to simulate dispersal and examine the resulting recruitment dynamics. Specifically, we used the open-source par-

ticle tracking platform Connectivity Modeling System (CMS; Paris et al. 2013), which combines reproductive ecology and larval biology with models of oceanic currents, to transport virtual larvae through time and space. Within CMS, we modeled scamp life history, released virtual larvae from spawning locations throughout US waters, and tracked their simulated movements from spawning grounds to settlement locations. These simulations can inform the degree of connectivity between fishery management units (Le Corre et al. 2019, 2020, Zeng et al. 2019). We focused on 3 topics: (1) whether oceanographic conditions in the region favor local retention or long-distance dispersal; (2) which spawning regions are likely to produce significant scamp recruitment; and (3) the degree of trans-boundary connectivity between the scamp stock units in the US Gulf of Mexico and Atlantic Ocean.

2. MATERIALS AND METHODS

2.1. Biophysical modeling framework

We used the CMS to simulate the spawning of virtual eggs from expected scamp spawning locations throughout the US Gulf of Mexico and Atlantic regions. CMS uses the output from oceanographic models to advect individual virtual larvae through time and space and monitors the trajectories of those larvae from spawning to settlement. In total, we conducted 8 different simulations, which used the same seasonal and spatial spawning distributions but differed in terms of the underlying ocean velocity fields and assumed larval traits and behaviors (Table 1). These 8 simulations can be thought of as one base simulation and 7 variations that explore 2 kinds of known uncertainty: that due to ocean circulation and that due to larval biology. In the subsequent sections, we describe the configuration of the base simulation we used to model scamp dispersal. Then, we describe how we modified this base simulation to investigate hydrodynamic and biological uncertainties, and the ensemble modeling approach we used to analyze the results and quantify scamp connectivity.

2.2. Initial conditions of the base biological model

2.2.1. Spawning time

To determine the timing of simulated spawning in CMS, we used a generalized additive model (GAM) to analyze the seasonality of all available reproductive histology data for scamp caught in the US Gulf of Mexico (1972–2017, National Marine Fisheries Service, Southeast Fisheries Science Center) and Atlantic (1976–2018, South Carolina Department of Marine Resources). After removing data without reliable positional information and years with fewer than 30 samples, these data included 5093 reproductive samples (Fig. S1, Table S1 in the Supplement at www.int-res.com/articles/suppl/m750p133_supp.pdf). Of these, 650 were obtained from females within approximately 24 h of spawning, with spawning observed at depths between 14 and 177 m. We used a binomial GAM to predict the probability that a sample came from a spawning female (η, Eqs. 1–3). The covariates we considered included average bottom depth (d), local change in bottom depth (*delta*), distance to the

Table 1. Scamp larval dispersal simulations (1 base simulation and 7 sensitivity simulations) investigating variation due to uncertainty in ocean velocity estimates and scamp larval biology. OVM (ontogenetic vertical migration): whether the simulation includes (Yes) or does not include (No) an ontogenetic shift in the vertical distribution of simulated larvae; H: simulations included in the hydrodynamic ensemble; B: simulations included in the biological ensemble; PLD: pelagic larval duration; HYCOM: Hybrid Coordinate Ocean Model; GOM: Gulf of Mexico; GOFS: Global Ocean Forecasting System; HiRes: high resolution; IAS: Inter-American Seas; SABGOM: South Atlantic Bight and Gulf of Mexico

Simulation	Hydrodynamic product	Competency period (PLD) (d)	OVM	Settlement criteria (m)	Ensemble
Base	HYCOM GOM + GOFS	33–52	No	30	H, B
GOM HiRes	HYCOM GOM HiRes + GOFS	33–52	No	30	H
IAS	HYCOM IAS	33–52	No	30	H
Mercator	Mercator	33–52	No	30	H
SABGOM	SABGOM	33–52	No	30	H
PLD 57	HYCOM GOM + GOFS	33–57	No	30	B
OVM	HYCOM GOM + GOFS	33–52	Yes	30	B
45 m	HYCOM GOM + GOFS	33–52	No	45	B

continental shelf-break (*dist*; Text S1), day of year (*doy*), year (*yr*), and whether the sample came from a fishery-dependent or fishery-independent source (*source*). We calculated the depth-based covariates from the Coastal Relief Model (National Geophysical Data Center 2023) using a 100 m radius around each catch location. Scamp are thought to spawn preferentially at high-relief rocky areas near the edge of the continental shelf (Coleman et al. 2011, SAFMC 2013, Farmer et al. 2017, Grüss et al. 2018); unfortunately, habitat, relief, and substrate data are not consistently available throughout our full study area. As these data are only available at select sites, we could not include them explicitly in this model. Instead, we used the change in depth within 100 m of each sample location as a proxy for local relief.

$$\eta \sim \text{Bernoulli}(\pi) \quad (1)$$

$$E(\eta) = \pi, \text{ and } \text{var}(\eta) = \pi \times (1 - \pi) \quad (2)$$

$$\begin{aligned}\text{logit}(\pi) = \alpha + s_1(doy^{\star}) + s_2(dist^{\dagger}) + s_3(d^{\dagger}) \\ + s_4[\log(delta^{\dagger})] + f_1(yr) + f_2(source)\end{aligned} \quad (3)$$

where η is the probability of scamp spawning, π is the probability of a spawning female and $(1 - \pi)$ is the probability of a male or non-spawning female; logit is the logit link function; α is the model intercept; s is a smoothed cubic spline function; f is a categorical function; * denotes temporal covariates that changed when predicting the spawning season; and † denotes spatial covariates that changed when predicting the spawning distribution.

For this and all subsequent GAMs, we used the 'mgcv' package (Wood 2011) in R version 4.0.5 (R Core Team 2023). We estimated smoothing parameters using restricted maximum likelihood and conducted variable selection with the 'select == TRUE' argument, which is the recommended method for GAMs and adds an additional penalty to each term so that they can be removed from the model during the fitting process (Marra & Wood 2011). The final model (Eq. 3) retained all variables and explained 45.1% of the deviance in spawning with an adjusted r^2 of 0.402. This model predicted a high probability of spawning from March through May, with a peak in April (Fig. 1A), which is consistent with previous reports of the scamp spawning season (Harris et al. 2002, Lombardi-Carlson et al. 2012, Farmer et al. 2017).

There has not been sufficient histology sampling to estimate a different spawning season for each year (Table S1); therefore, we used this average seasonality to distribute simulated spawning events throughout the year. First, we delineated the spawning season by calculating the middle 95% of the area under the spawning season curve from the model (Fig. 1A) and only simulated scamp spawning between *doy* 55 (late February) and 165 (mid-June). Then, within this spawning season, we simulated spawning every other day and scaled the number of virtual eggs spawned on each day to be proportional to the predicted probability of spawning on that day. In this way, we simulated more spawning in April, when our model and other reports suggest scamp spawning is higher than at the beginning or end of the estimated spawning season.

2.2.2. Spawning location

We used a similar approach to scale the spatial distribution of simulated spawning throughout the US Gulf of Mexico and Atlantic. Briefly, using a grid of locations spaced at 10 km intervals, we calculated the expected spawning (λ) as the product of spatial predictions from 3 statistical models (Eq. 4): the probability of scamp presence, the estimated abundance when present, and the probability of spawning when present. Then, we simulated spawning at each grid location but spawned more virtual larvae at locations where these models predicted higher spawning (Fig. 1B).

$$\lambda = \beta \times \mu \times \eta \quad (4)$$

where β is the probability of scamp presence; μ is the estimated scamp abundance, when present; and η is the probability of scamp spawning, when present (Eq. 2).

In effect, this (Eq. 4) builds a species distribution map and then uses the histology-based spawning model we described above (Eq. 3) to adjust where the simulated spawning is concentrated with respect to depth, local change in depth (a proxy for local relief), and proximity to the edge of the continental shelf. Therefore, if scamp tend to spawn closer to the shelf edge or at different depths than the species distribution in general, our modeling approach can readily account for this difference.

To build the species distribution map, we used a common delta model approach (also known as a hurdle model) to analyze recent data (2011–2017) from 5 fishery-independent surveys (see Text S2 for full details). Sampling for these surveys occurs largely from May through August, so it does not perfectly align with the scamp spawning season (March through May). However, these are the best available data to inform the relative abundance of scamp throughout US waters, which is necessary to appropriately scale the magnitude of simulated spawning. Moreover, there is no evidence that scamp travel long distances to

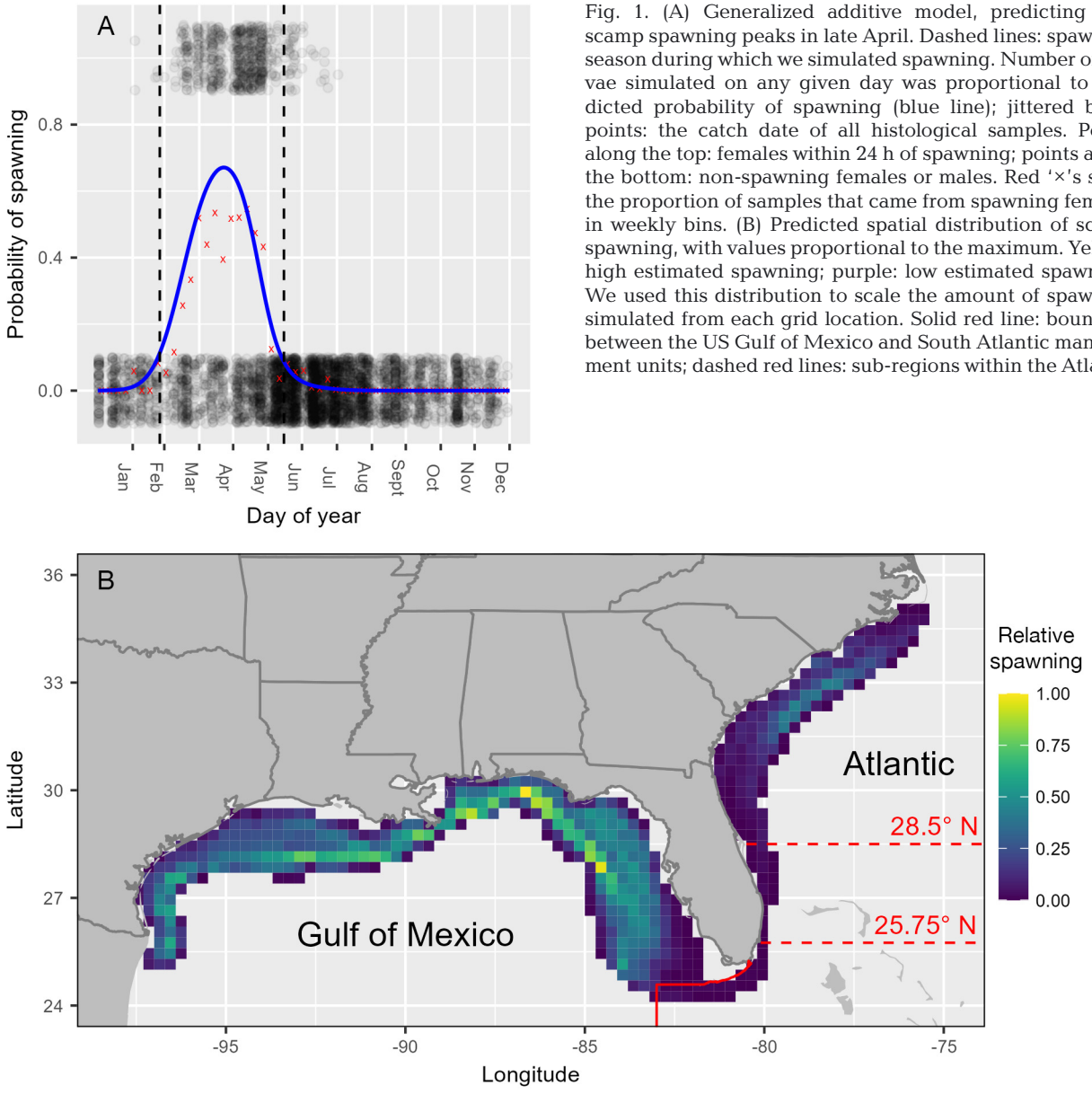

Fig. 1. (A) Generalized additive model, predicting that scamp spawning peaks in late April. Dashed lines: spawning season during which we simulated spawning. Number of larvae simulated on any given day was proportional to predicted probability of spawning (blue line); jittered black points: the catch date of all histological samples. Points along the top: females within 24 h of spawning; points along the bottom: non-spawning females or males. Red '×'s show the proportion of samples that came from spawning females in weekly bins. (B) Predicted spatial distribution of scamp spawning, with values proportional to the maximum. Yellow: high estimated spawning; purple: low estimated spawning. We used this distribution to scale the amount of spawning simulated from each grid location. Solid red line: boundary between the US Gulf of Mexico and South Atlantic management units; dashed red lines: sub-regions within the Atlantic

spawn, and by including a histology model, our approach accounted for potential inshore–offshore shifts in the spawning distribution compared to the species distribution.

The delta model approach we used to estimate the species distribution map included 2 GAMs: a binomial sub-model that predicted the probability of scamp presence (β; Eqs. 5–7) and a Gaussian sub-model that predicted scamp abundance when present (μ; Eq. 8). Both sub-models had the same set of covariates, which included all covariates that overlapped across the surveys: *d*, *delta* (as a proxy for local relief), *dist* (Text S1), position along the shelf break (*pos*; Text S1), percent observed substrate (*sub*), observed maximum relief (*rel*), year (*yr*), and survey program (*survey*).

$$\beta \sim \text{Bernoulli}(\theta) \tag{5}$$

$$E(\beta) = \theta \text{ and } \text{var}(\beta) = \theta \times (1 - \theta) \tag{6}$$

$$\begin{aligned}\text{logit}(\theta) = \alpha + s_1(dist^{\dagger}) + s_2(pos^{\dagger}) + s_3(d^{\dagger}) \\ + s_4[\log(delta^{\dagger})] + s_5(sub) + f_1(yr) \\ + f_2(survey) + f_3(rel)\end{aligned} \tag{7}$$

$$\begin{aligned}\sqrt[4]{\mu} = \alpha + s_1(dist^{\dagger}) + s_2(pos^{\dagger}) + s_3(d^{\dagger}) + s_4[\log(delta^{\dagger})] \\ + s_5(sub) + f_1(yr) + f_2(survey) + f_3(rel)\end{aligned} \tag{8}$$

where θ is the probability of scamp presence and (1 − θ) is the probability of absence; Eq. (7) uses all visual survey data to predict the probability of scamp presence, and Eq. (8) uses 4th-root-transformed positive count data and a Gaussian error distribution to estimate scamp abundance when present.

The binomial sub-model explained 25.6% of the deviance in whether a survey observed scamp, with an adjusted r^2 of 0.238. The Gaussian sub-model explained 26.2% of the deviance in survey counts (when scamp were present), with an adjusted r^2 of 0.254.

We used the spatial predictions of these 2 sub-models, in combination with the spatial predictions from the previously described histology model (Eq. 3), to estimate the spatial distribution of scamp spawning (Fig. 1B). Specifically, we generated a grid of locations spaced at 10 km intervals throughout the US Gulf of Mexico and Atlantic, and at each location, we used the spatial covariates in each model (e.g. depth, denoted by †) to predict the probability of scamp presence (β; Eqs. 5–7), scamp abundance when present (μ; Eq. 8), and the probability of scamp spawning when present (η; Eq. 3). The product of these 3 predictions (Eq. 4) estimates the relative amount of scamp spawning at each grid location. These models suggest that scamp are most likely to spawn around 75 m depth (Fig. S5) and at locations near the edge of the continental shelf (Fig. 1B), which is consistent with previous reports of scamp spawning (Coleman et al. 2011, SAFMC 2013, Farmer et al. 2017, Grüss et al. 2018).

Unfortunately, observations of relief and substrate are not available throughout our full study area. Therefore, we could not include these spatial covariates in our spawning model or use them to predict the species distribution. Instead, we used the local change in depth within a 100 m radius of each location as a proxy for local relief. In addition, we used the survey observations of percent available substrate and maximum relief as controlling variables in our species distribution modeling to better estimate the relationship between scamp abundance and the other spatial covariates in the model (e.g. depth). Therefore, our spatial models likely captured the broad spatial patterns in scamp spawning but they cannot account for spatial variation at fine scales.

In addition, there is not enough empirical data to estimate annual spawning maps. Instead, we used data from multiple years to inform an average spatial distribution that we applied for all simulation years. This average distribution analyzed recent survey data to estimate the relative abundance of scamp and combined it with histology samples that were collected over a longer time period. Therefore, the exact spawning locations of scamp and how they might change over time remain uncertain.

To confine the spatial extent of spawning locations, we calculated the middle 95% of the area under the depth marginal effect of all 3 models combined (Fig. S5). As a result, we simulated spawning at grid locations with an average depth between 14 and 279 m. Then, we scaled the number of virtual eggs spawned at each grid location to be proportional to the predicted probability of spawning at that location (Fig. 1B), which was highest near the edge of the continental shelf. This is consistent with previous reports (Coleman et al. 2011, SAFMC 2013, Farmer et al. 2017, Grüss et al. 2018) and the empirical depth range of spawning observed in the histology data (14–177 m, with most spawning between 50 and 100 m).

2.2.3. Scaling the magnitude of spawning

For each year, we simulated approximately 100 000 virtual eggs, a number we chose through a resampling analysis of preliminary results (Text S3). To calculate the number of eggs spawned at each time and place, we first used the histology model (Eq. 3) to distribute the 100 000 eggs throughout the spawning season (Fig. 1A). Then, on each spawning day, we used the spatial distribution (Fig. 1B) based on all 3 models combined (Eq. 4) to allocate the eggs to each grid location. Finally, we rounded the number of eggs for each spawning event (combination of time and place) to the nearest whole number. After rounding, we simulated 99 102 eggs yr^{-1} and used the same temporal and spatial distribution for each year of our 8 simulations (base and 7 sensitivity simulations). In total, we simulated the spawning of 3 765 876 virtual eggs.

We simulated spawning every other day during the spawning season; however, for computational efficiency, we did not spawn eggs from all locations every time. Instead, we randomly assigned spawning locations to one of 5 groups and spawned eggs from each group on a different set of dates (Fig. S7). For example, at locations in one group, we simulated spawning on *doy* 55, 65, 75, etc., but at nearby locations in another group, we simulated spawning on *doy* 57, 67, 77, etc. In this way, only 20% of the locations simulated spawning on each day, with spawning occurring at individual locations every 10 d. This approach maintained the temporal and spatial resolution needed for robust probabilistic results but reduced the total number of virtual eggs required for each simulation, which is important for computational efficiency.

2.2.4. Vertical distribution of eggs and larvae

We simulated spawning 10 m above the sea floor, which is consistent with the depth range in which scamp courtship behavior has been observed (Gilmore & Jones 1992, Schobernd & Sedberry 2009). Immediately after spawning, the simulated eggs float to the surface, as is consistent with grouper eggs. The exact rate at which scamp eggs float is unknown, so we specified that simulated eggs float to the surface over the first 9 h and then remain in the top 15 m of the water column until they hatch. We defined this assumption through a series of initial simulations that also confirmed that the resulting connectivity patterns were similar under a wide range of buoyancy assumptions (Text S4). After 2 d, when grouper eggs typically hatch (Roberts & Schlieder 1983, Colin et al. 1996), the simulated larvae undergo vertical migration, with depths determined probabilistically (Table 2). For the base simulation, we used one vertical distribution throughout the entire larval duration (Table 2: 'no ontogenetic shift'). We informed the assumed vertical distribution of simulated larvae by analyzing the limited empirical data available for grouper larvae caught during the scamp spawning season (Text S4). Because these data are limited, however, the exact vertical distribution of scamp larvae is uncertain.

2.2.5. Settlement

We only allowed virtual larvae to settle successfully when certain criteria were met. First, we specified the settlement competency period from 33 to 52 d. Because the PLD of scamp remains unknown, we approximated it using information on congeneric gag grouper *Mycteroperca microlepis* larvae in the study region (Fitzhugh et al. 2005, Adamski et al. 2012), which tend to settle between 33 and 52 d old (Text S5). These values are also consistent with the PLD of another closely related species, black grouper *M. bonaci* (Keener et al. 1988).

Second, we used 30 m as a boundary for suitable settlement habitat (see below) and only considered virtual larvae to have successfully settled if they reached a depth <30 m when they were between 33 and 52 d old. If a simulated larva reached 33 d old and was not in a suitable settlement habitat (i.e. depth <30 m), then it continued to move until it either encountered settlement habitat or reached the maximum PLD (52 d), at which point it stopped and we considered it dead.

Little is known about the settlement preferences of scamp, but larvae are not known to require a specific nursery habitat, and juveniles are thought to inhabit reefs between 20 and 30 m depth (Coleman et al. 2011). This is consistent with the few data available for age-0 and age-1 scamp caught in the northeastern Gulf of Mexico, which suggest that young scamp are predominantly caught at depths of <30 m (Fig. S9). In addition, surveys that sample depths <30 m, like those in the Florida Keys (Keller et al. 2020), tend to record a higher proportion of small scamp than do surveys that operate in deeper waters (Thompson et al. 2020). Therefore, we felt that using a depth-based settlement criteria of 30 m was appropriate.

To delineate settlement habitat, we extracted the 0 and 30 m isobaths from the global 30 arc-second bathymetry grid available from GEBCO (General Bathymetric Chart of the Oceans; www.gebco.net) and defined suitable settlement habitat as all areas between these isobaths on the US Gulf and Atlantic continental shelves. This does not account for potential spatiotemporal variation in settlement habitat, which is not well understood for scamp and is beyond the scope of this study. It also assumes that scamp larvae can either settle anywhere shallower than 30 m or that once near their preferred settlement habitat (yet unknown), larvae can direct their swimming to increase the likelihood of finding it. These are reasonable assumptions given the lack of information on scamp settlement and that many fish larvae can alter their behavior to facilitate settlement (Montgomery et al. 2001, Kingsford et al. 2002, Gerlach et al. 2007, Bottesch et al. 2016, Teodósio et al. 2016, Faillettaz et al. 2018).

Hereafter, we use terms such as settlement, successful larvae, and settlers to refer to virtual larvae that found suitable settlement habitat during the

Table 2. Percentage of simulated scamp larvae in each depth bin for each of 2 vertical distribution assumptions. Most simulations assumed a single vertical distribution throughout the entire pelagic larval duration (PLD); one sensitivity simulation assumed an ontogenetic shift in the vertical distribution of larvae. Connectivity Modeling System uses these distributions, which we calculated by analyzing empirical data (Text S4), to specify the vertical distribution of simulated larvae in each timestep

Depth bin (m)	No ontogenetic shift	Ontogenetic shift	
	Entire PLD	Pre-flexion	Post-flexion
0–20	60	64	40
20–40	30	28	48
40–60	10	8	12
60–100	0	0	0

competency period instead of reaching their maximum PLD in deeper waters. Similarly, for fluency, we sometimes use terms like recruit or recruitment interchangeably with settler or settlement, even though our simulations do not model post-settlement processes that influence whether settled larvae ultimately recruit to the population as juveniles.

2.3. Exploring known uncertainties

There are several sources of uncertainty that we know will influence the trajectories of simulated larvae and, therefore, our estimates of scamp connectivity. Different hydrodynamic models produce different current velocity estimates, and several areas of scamp larval ecology are relatively understudied. Therefore, we conducted 7 additional simulations that use alternative assumptions for the ocean velocity estimates, PLD, settlement habitat, and vertical distribution of larvae. These are analogous to sensitivity analyses often used in stock assessment, or robustness trials often discussed for management strategy evaluation (Punt et al. 2016).

2.3.1. Ocean velocity fields

A large source of uncertainty in simulating larval dispersal is the variability between the estimated velocity fields from different hydrodynamic products (Karnauskas et al. 2022). Therefore, we conducted 5 simulations, including the base simulation, that assumed the same biological parameterization described above (i.e. spawning distribution, vertical distribution of eggs and larvae, and settlement criteria) but used velocity fields from different hydrodynamic products to transport the simulated larvae.

In total, we used velocity fields from 6 hydrodynamic products, but one was only used as a nest for others that did not cover our entire study area. These products were obtained from different ocean circulation models as well as implementations with a range of spatial and temporal resolutions, forcings, and data assimilation approaches (summarized in Table 3, details in Text S6). Note that we do not prefer any one hydrodynamic model over the others. Instead, we gave them equal weight when analyzing our results (see Section 2.4.2) and only refer to a base simulation for clarity in describing our methods.

Briefly, we used velocity fields from (1) the Hybrid Coordinate Ocean Model (HYCOM) Gulf of Mexico 1/25° analysis (hereafter GOM HYCOM), (2) the HYCOM Gulf of Mexico 1/50° analysis (hereafter GOM HYCOM HiRes; Le Hénaff & Kourafalou 2016), (3) the HYCOM Intra-American Seas 1/32° analysis (hereafter HYCOM IAS), (4) the Mercator GLORYS12V1 1/12° reanalysis (hereafter Mercator; Lellouche et al. 2021), and (5) the South Atlantic Bight and Gulf of Mexico 1/25° model (hereafter SABGOM; Hyun & He 2010, Xue et al. 2015). Two velocity fields (GOM HYCOM and GOM HYCOM HiRes) do not extend north of 32° N. Therefore, to cover our entire study area we nested them within (6) the operational 1/12° global HYCOM Global Ocean Forecasting System (hereafter HYCOM GOFS; Chassignet et al. 2007), which provides the boundary conditions for both GOM HYCOM and GOM HYCOM HiRes. For all hydrodynamic products, we used velocity fields at daily intervals.

Each product is available for different years and, thus, simulations using individual velocity fields do not always overlap (Table 3). However, the purpose of this study is to estimate probabilistic connectivity and

Table 3. Hydrodynamic product specifications. Our simulations used ocean velocity fields from 6 different hydrodynamic products with varying specifications. See Table 1 for product abbreviations and how these fields were applied across the simulations. Note that the GOFS fields were only used as a nest for other products that did not cover the entire region of interest. See Text S6 for details of each hydrodynamic product. CMS: Connectivity Modeling System

Hydrodynamic product		Years	Vertical resolution (top 100 m) (layers)	Horizontal resolution	Type of product	CMS diffusivity coefficient ($m^2 s^{-1}$)
HYCOM GOM		2012, 2013, 2015–2018	20	1/25° (ca. 4 km)	Hindcast	15
HYCOM GOM HiRes		2011–2017	11	1/50° (ca. 2 km)	Hindcast	12
HYCOM IAS		2010	7	1/32° (ca. 3.5 km)	Reanalysis	15
MERCATOR		2013–2017	22	1/12° (ca. 8 km)	Reanalysis	20
SABGOM		2004–2010	20	1/25° (ca. 4 km)	Hindcast	20
GOFS	Expt. 3.0	2011–2014	7	1/12° (ca. 8 km)	Hindcast	20
	Expt. 3.1	2015–2018	20			

recruitment patterns over time, not to produce a hindcast of recruitment in specific years. Therefore, we aimed to capture the interannual variability within each hydrodynamic product by using at least 5 yr of velocity fields (except for HYCOM IAS). This ensured that our results were probabilistically robust and allowed us to compare the general connectivity trends from simulations that use non-overlapping years (Karnauskas et al. 2022).

To account for processes not resolved by the resolution of the hydrodynamic products (sub-grid scales), we used the random walk displacement algorithm in CMS. It adds a random component to the motion of virtual larvae and approximates diffusion. The diffusivity values we used to scale the random walk ranged from 12 to 20 $m^2 s^{-1}$, with the value depending on the horizontal resolution of the ocean velocity field and Okubo's (1971) parameterization. However, SABGOM has lower eddy kinetic energy, and therefore variability, than other models (Fig. S10). Thus, after unpublished sensitivity explorations by Karnauskas et al. (2022), we used a slightly higher diffusivity value for SABGOM than for other models with the same horizontal resolution to ensure that our results captured a probabilistic distribution of dispersal pathways.

2.3.2. Biological traits

There is also uncertainty in several aspects of scamp larval biology and behavior. Specifically, little is known about the PLD of scamp, how the vertical distribution of scamp larvae changes throughout ontogeny, or the preferred settlement habitat of scamp. However, in contrast to the hydrodynamic models, of which none are preferred, the base model (Section 2.2, Table 1) does in fact represent our best assessment of the relevant scamp biology and behavior. To investigate how uncertainty in these traits might influence our results, we conducted 3 additional simulations that vary each trait, one at a time (Table 1). One extended the PLD to 57 d, which is the 97.5% quantile of settlement age for gag larvae in the Atlantic (Adamski et al. 2012); the second incorporated an ontogenetic shift in the vertical distribution of larvae (Table 2: 'ontogenetic shift'); and the third expanded the settlement criteria to 45 m. All 4 simulations (base and 3 biological variations) used the same temporal and spatial spawning distribution as well as the same ocean velocity fields (GOM HYCOM nested within GOFS).

2.4. Data analysis

2.4.1. Metrics and plots

To investigate the general patterns of scamp connectivity, we used 2 graphical approaches. First, we visualized connectivity matrices, which aggregate successfully settled larvae based on where they spawned and where they settled (see Fig. 2). These plots provide a convenient way to determine whether most larvae are likely to settle close to where they started (i.e. local retention as defined by Botsford et al. 2009) or disperse longer distances. Second, we mapped the spatial distribution of where successfully settled larvae spawned and settled (see Fig. 3). These maps help to identify important spawning locations that are likely to be strong sources of recruitment to the broader region and settlement locations that are likely to be recruitment hotspots, collecting larvae from widespread spawning locations.

In addition to these general patterns of connectivity, we specifically focus on the connectivity dynamics between the US Gulf of Mexico and Atlantic regions. To delineate the 2 regions, we used the jurisdictions of the Gulf of Mexico and South Atlantic Fisheries Management Councils. Because the jurisdictions of these management bodies do not apply within state waters (3 nautical miles [ca. 5.6 km] from shore), we approximated a boundary between them in a way that can be applied to any location, including those within state waters. Our boundary (shown in Fig. 1B) follows US Highway 1 from Miami, Florida, to Key West, Florida, until it intersects latitude 24° 35' N, which it follows west until it intersects longitude 83° W, which it follows south. We considered all spawning and settlement habitat north and west of this line to be in the Gulf of Mexico and all habitat south and east of this line to be in the Atlantic. We also further partitioned the US Atlantic into subregions at latitude 25.75° N (approximately Miami, Florida) and latitude 28.5° N (approximately Cape Canaveral, Florida). Using these geographic boundaries, we calculated a set of proportions to describe the trans-regional connectivity patterns in the area, including what percent of recruits settling in the Atlantic came from the Gulf of Mexico.

2.4.2. Ensemble models

In general, we report the findings of a hydrodynamic ensemble, a biological ensemble, and an overall ensemble. The hydrodynamic ensemble combines and summarizes the results of 5 simulations: the base

simulation and the 4 variations that change the underlying ocean velocity field. The biological ensemble combines and summarizes the results of 4 simulations: the base simulation and the 3 variations that change the larval biology and behavior. The overall ensemble combines and summarizes the results of all 8 simulations together (base and 7 sensitivity simulations).

For the raster maps and the connectivity matrix plots, which use spatial polygons (Fig. S11) to aggregate successful recruits, we first calculated the result of interest (e.g. number of successfully settled particles spawned in a particular area) for each simulation and normalized it by the total number of virtual larvae spawned in the same simulation (Eq. 9). Then, for each raster cell or matrix element, we calculated the arithmetic mean across the simulations in each ensemble (Eq. 10). Finally, for plotting, we normalized the mean values so that they are proportional to the maximum.

$$N_s[i,j] = \frac{\sum n_{s,i,j}}{T_s} \quad (9)$$

where

$$n_{s,i,j} = \begin{cases} \text{Recruits spawned in polygon } i \text{ and settled in polygon } j \text{ for simulation } s \text{ (Fig. 2)} \\ \text{Recruits spawned from raster cell } [i,j] \text{ for simulation } s \text{ (Fig. 3A)} \\ \text{Recruits settled in raster cell } [i,j] \text{ for simulation } s \text{ (Fig. 3B)} \end{cases}$$

and T is the total number of larvae spawned in simulation s

$$\overline{N_E}[i,j] = \frac{1}{k_E} \sum_{s \in E} N_s[i,j] \quad (10)$$

where E is an ensemble of simulations and k_E is the number of simulations in the ensemble.

For the proportions (e.g. percentage of Atlantic recruits from Gulf of Mexico spawning areas), we resampled each simulation 1000 times and calculated every proportion for each resample. Then, we pooled the resampled proportions from all the simulations in an ensemble before calculating the ensemble mean and standard deviation. This captures the uncertainty within each simulation as well as across the simulations in an ensemble. We also, however, examined the results for each simulation individually and highlight major differences when relevant.

3. RESULTS

On broad spatial scales, we found a predominant pattern of local retention (Botsford et al. 2009), with most settled larvae ending near their spawning location (Fig. 2). Across all simulations, most potential recruits (i.e. virtual larvae that found settlement habitat) started in the eastern Gulf of Mexico (Fig. 3A), with a peak off the west coast of Florida near 28° N. This area was also the most successful settlement area, with the highest number of potential recruits settling off the west coast of Florida near 28° N (Fig. 3B). In general, the high degree of local retention persisted across all 8 simulations (Fig. S12), but the spawning and settlement locations of potential recruits were more spatially distributed across the

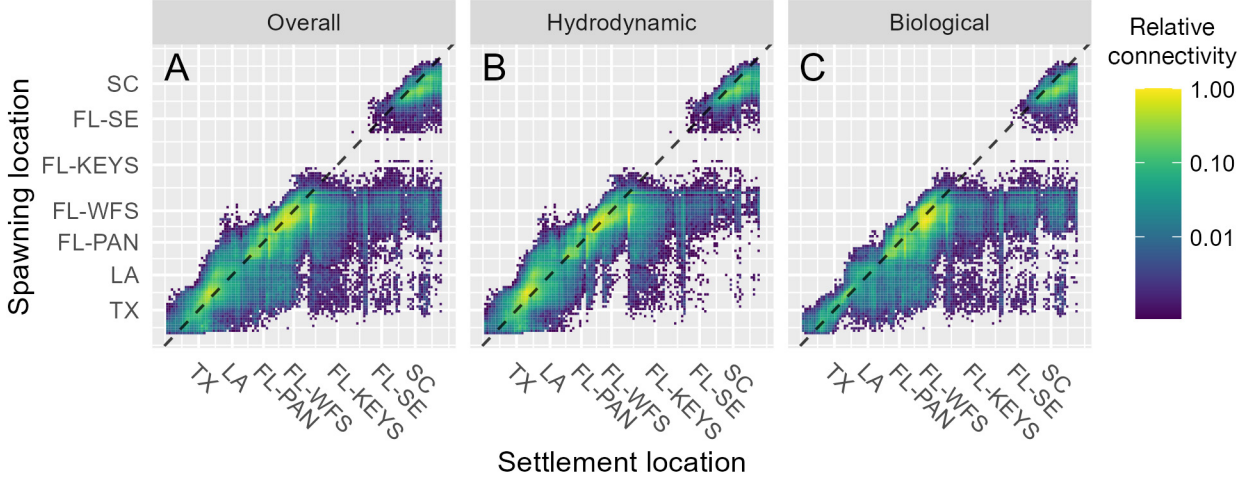

Fig. 2. Connectivity matrices showing the dispersal dynamics of successful simulated scamp larvae summarized over the (A) overall, (B) hydrodynamic, and (C) biological ensembles. Spawning and settlement locations of successful virtual larvae are shown. Values (on a log scale) are proportional to the maximum across all panels; yellow: high estimated connectivity; purple: low estimated connectivity. Black dashed line: axis of local retention (i.e. settlement location = spawning location; Botsford et al. 2009). TX: Texas; LA: Louisiana; FL-PAN: Florida Panhandle; FL-WFS: West Florida Shelf; FL-KEYS: Florida Keys; FL-SE: Atlantic coast of Florida; SC: South Carolina. These geographic sub-regions follow the US coastline from west to east and are identified in Fig. S7; Fig. S12 shows a similar connectivity matrix for each individual simulation

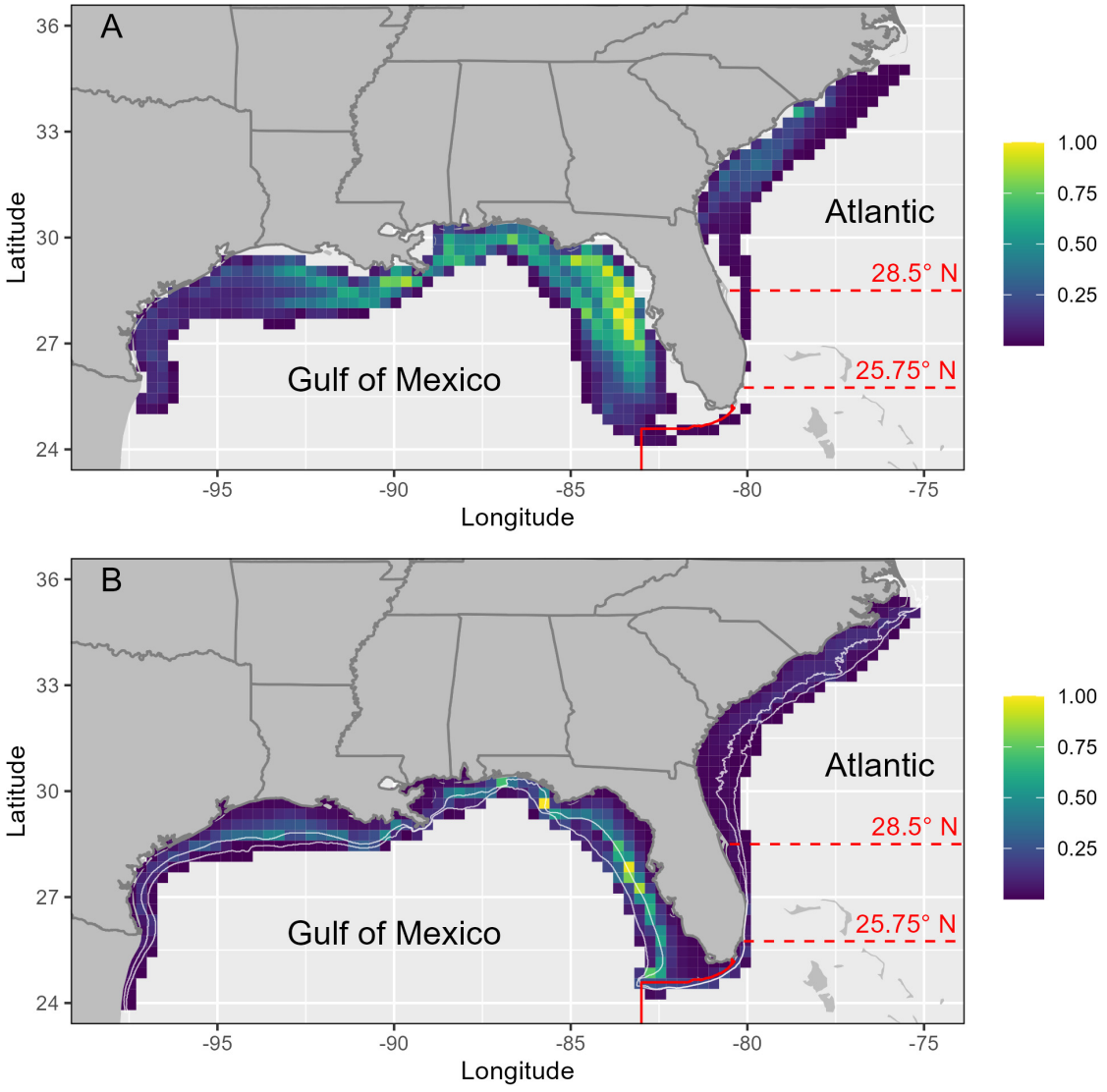

Fig. 3. Spatial distribution of (A) spawning and (B) settlement locations of simulated scamp larvae that successfully settled. Values are proportional to the maximum; yellow: areas where many successful virtual were spawned or settled; purple: areas where few successful larvae were spawned or settled. Maps show results from the overall ensemble that pooled all simulations. Figs. S13 & S14 show the hydrodynamic and biological ensembles individually. Solid red line: boundary between the US Gulf of Mexico and Atlantic management units; dashed red lines: sub-regions within the Atlantic; white lines in (B) represent 2 alternative assumptions for settlement habitat. For the base simulation, settlement habitat included any location between the coastline and the 30 m isobath. For one of the sensitivity analyses, settlement habitat was extended to the 45 m isobath

northern Gulf of Mexico when the results were summarized over the simulations in the hydrodynamic ensemble than when summarized over the simulations in the biological ensemble (Figs. S13 & S14).

Despite this trend of high local retention, we also found that more than one-third of virtual scamp larvae settling in the US Atlantic region came from the Gulf of Mexico (Fig. 4). Almost 65% of these larvae, which were transported from the Gulf to the Atlantic, settled in the Florida Keys — technically in the Atlantic, but very close to the boundary between the 2 regions. To more conservatively estimate the contribution that Gulf of Mexico spawning makes to recruitment in the Atlantic, we also report the results when we only consider those potential recruits that settled farther into the Atlantic (i.e. north of latitude 25.75° N, or north of latitude 28.5° N). Even then, 17% of the larvae that settled north of latitude 25.75° N (Miami) and 10% of the larvae that settled north of latitude 28.5° N (Cape Canaveral) started in the Gulf of Mexico (Table 4). There is, however, considerable variation in these proportions, both between simula-

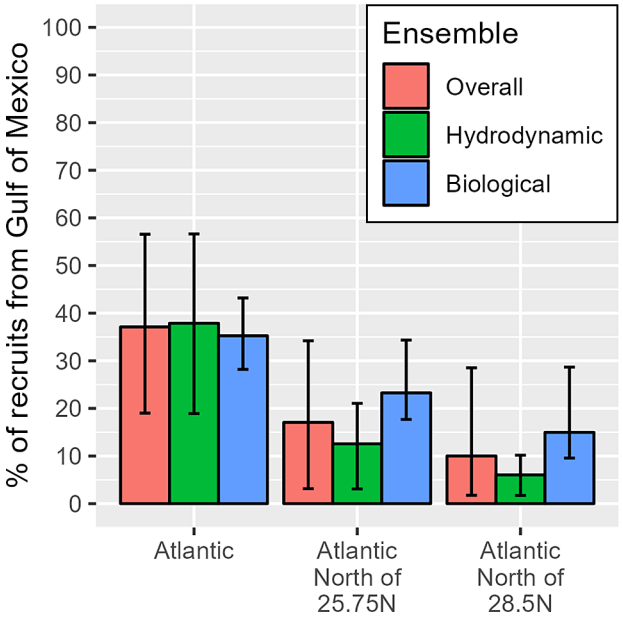

Fig. 4. Percentage of scamp recruits to the Atlantic that came from the Gulf of Mexico. We resampled each simulation 1000 times and calculated the proportion for each resample then pooled the resampled proportions from the simulations in an ensemble and calculated the ensemble mean (bars) and SD (error bars). This captures the uncertainty within each simulation as well as across the simulations in an ensemble

tions and between years within a simulation (Table 4, Fig. 5).

The percentage of potential Atlantic recruits (i.e. virtual larvae that settled anywhere in the Atlantic) that came from the Gulf of Mexico is sensitive to the biological parameterization of our simulations (e.g. PLD, settlement criteria, vertical distribution). The differences are greater, however, when we compare simulations that use the same biological parameterization but rely on current velocity estimates from different oceanographic models. For example, the simulation using SABGOM estimated that 19% of potential Atlantic recruits started in the Gulf (year-to-year values range from 12 to 35%; Table 5), while the simulation using the high-resolution HYCOM model estimated that 56% of potential Atlantic recruits started in the Gulf (year-to-year values range from 29 to 74%; Table 5). In contrast, the values from simulations in the biological ensemble, which all use the same hydrodynamic model, only range from 29 to 43%. There is still, however, considerable year-to-year variability within each simulation (Fig. 5).

This relationship changes when we focus on larvae that settled farther north in the Atlantic. Specifically, the percentage of potential Atlantic recruits that settled north of latitude 28.5° N (Cape Canaveral) but came from the Gulf is more sensitive to the biological specifications of a simulation than to the hydrodynamic model used. For example, in the base simulation, 10% of larvae that settled north of Cape Canaveral started in the Gulf of Mexico. However, when the suitable settlement habitat was extended from depths of <30 m to depths <45 m, 28% of the larvae that settled north of Cape Canaveral came from the Gulf of Mexico. By contrast, the percentage of potential recruits north of Cape Canaveral that came from the Gulf remained relatively consistent across the simulations in the hydrodynamic ensemble, which all used the same biological parameterization as the base simulation (2–10%; Table 4).

Larvae that left the Gulf of Mexico and settled in the Atlantic came overwhelmingly from the West Florida Shelf (Fig. 6). When we focus only on poten-

Table 4. All proportions by simulation. We calculated several proportions to describe the scamp connectivity dynamics between the US Gulf of Mexico (GOM) and Atlantic (ATL). Columns 2–4 describe what percentage of recruits to various portions of the Atlantic came from spawning in the Gulf of Mexico. Columns 5 and 6 describe what percentage of simulated larvae from each region successfully settled anywhere. The last column describes what percentage of successful larvae spawned from Gulf of Mexico spawning areas settled in the Atlantic. See Table 1 for abbreviation definitions

Simulation (ensemble)	% ATL recruits from GOM	% ATL recruits (N of 25.75°) from GOM	% ATL recruits (N of 28.5°) from GOM	% ATL Spawn Settled	% GOM Spawn Settled	% GOM to ATL
Base (H, B)	34	19	10	25	26	7
GOM HiRes (H)	56	21	9	39	26	11
IAS (H)	25	9	5	32	27	4
Mercator (H)	55	11	4	31	23	11
SABGOM (H)	19	3	2	27	20	2
PLD 57 (B)	36	22	12	27	27	7
OVM (B)	29	18	10	19	32	9
45 m (B)	43	34	28	41	30	7

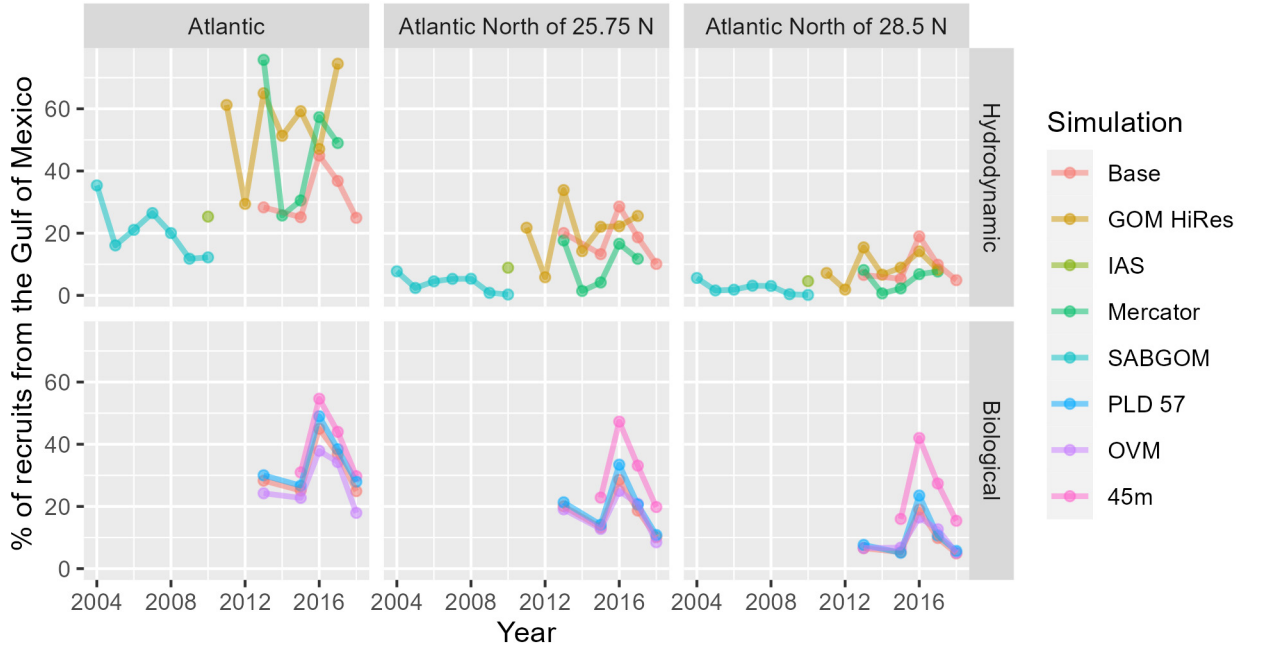

Fig. 5. Percentage of scamp recruits to the Atlantic that come from the Gulf of Mexico by simulation and year. Top row: hydrodynamic ensemble simulations; bottom row: biological ensemble simulations. Note that the 'base' simulation is in both ensembles. Lines connecting data points do not represent a regression or trend and are only included to highlight the year-to-year changes within a simulation. Each column shows the proportion based on recruitment to a different portion of the Atlantic

Table 5. Percentage of scamp recruits to the US Atlantic that came from Gulf of Mexico spawning locations. Dashes indicate that the simulation was not conducted for that year. See Table 1 for abbreviation definitions

Year	Base (H, B)	GOM HiRes (H)	IAS (H)	Mercator (H)	SABGOM (H)	PLD 57 (B)	OVM (B)	45 m (B)
2004	–	–	–	–	35	–	–	–
2005	–	–	–	–	16	–	–	–
2006	–	–	–	–	21	–	–	–
2007	–	–	–	–	26	–	–	–
2008	–	–	–	–	20	–	–	–
2009	–	–	–	–	12	–	–	–
2010	–	–	25	–	12	–	–	–
2011	–	61	–	–	–	–	–	–
2012	–	29	–	–	–	–	–	–
2013	28	65	–	76	–	30	24	–
2014	–	51	–	26	–	–	–	–
2015	25	59	–	31	–	27	23	31
2016	45	47	–	57	–	49	38	55
2017	37	74	–	49	–	38	34	44
2018	25	–	–	–	–	28	18	30
All	34	56	25	55	19	36	29	43

tial recruits that settled farther into the Atlantic, north of latitude 25.75° N (Miami), the spawning locations of these trans-regional settlers were limited largely to the southern portion of the West Florida Shelf. This southern concentration is even more extreme when we focus only on potential recruits that settled north of latitude 28.5° N (Cape Canaveral).

4. DISCUSSION

Consistent with expectation (Jones et al. 2005, Cowen et al. 2006, Buston et al. 2012, Almany et al. 2013, Vaz et al. 2023), we found that scamp dispersal largely followed a pattern of local retention (Fig. 2). Most virtual larvae in our simulations settled close to

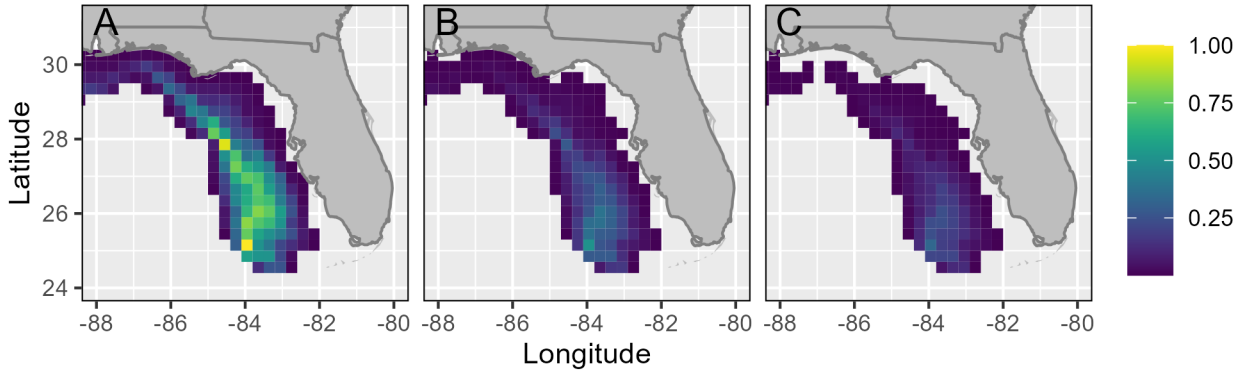

Fig. 6. Distribution of the spawning locations for Atlantic scamp recruits that came from the Gulf of Mexico and ended in a different portion of the Atlantic: (A) the entire Atlantic, (B) north of 25.75° N, and (C) north of 28.5° N. Values are proportional to the maximum across all panels. Yellow: spawning areas that produced a high number of Gulf to Atlantic recruits; purple: spawning areas that produced a low number of Gulf to Atlantic recruits. Maps show results from the overall ensemble that pooled all simulations

their spawning sites. However, there was also a consistent pattern of some larvae dispersing away from the natal place. Notably, although most larvae from the West Florida Shelf settled there, some dispersed to the Florida Keys and along the Atlantic shelf, even as far north as North Carolina (Fig. 2). Even if not predominant, this pattern of consistent long-distance dispersal has important ramifications for the connectivity dynamics, genetic structure, and fishery management of scamp.

Specifically, we found that approximately one-third of potential scamp recruits to the Atlantic came from the Gulf of Mexico (Fig. 4). Most of these recruits that left the Gulf of Mexico settled in the Florida Keys, but even when we only considered potential Atlantic recruits settling north of latitude 25.75° N (Miami, Florida), Gulf of Mexico spawning still accounted for 17% of Atlantic recruitment. This external recruitment might increase the resilience of the scamp population in the US Atlantic. In addition, this degree of connectivity appears to provide sufficient trans-regional mixing to minimize spatial patterns in the genetic structure of scamp populations (Zatcoff et al. 2004).

It is important to note that demographic connectivity examines unique events of individuals moving between regions, while genetic connectivity studies unveil patterns that occur over multiple generations and evolutionary timescales (Carr et al. 2017, Legrand et al. 2022, Vaz et al. 2022). Our results suggest a recurring pattern of transport from the Gulf of Mexico to the Atlantic Ocean, which, if consistent over long timescales, can explain the observed genetic structure of scamp populations in the region — particularly if we consider the possibility of multi-generational transport, which has been shown to better predict spatial patterns in genetic differentiation than single-generation transport models or conventional conceptual models like isolation-by-distance (Legrand et al. 2022).

Dispersal over multiple generations can magnify the effects of demographic connectivity and reconcile mismatches in the spatial scale of demographic and genetic connectivity through 2 mechanisms (Legrand et al. 2022). Filial connectivity traces explicit connections between parents and offspring (i.e. dispersal of single lineages over generations). Coalescent connectivity considers the implicit linkages between areas that have no demographic connectivity between them but share common ancestry because they receive dispersal from the same external area. Both filial and coalescent connectivity are important when considering how demographic connectivity pathways revealed by dispersal modeling may lead to observed patterns of genetic connectivity (Legrand et al. 2022).

For example, even if a particular individual does not move from the Gulf to the Atlantic, it may disperse downstream far enough such that when it reproduces as an adult, its larvae are more likely to move between the regions. Specifically, most potential Atlantic recruits from the Gulf of Mexico started on the West Florida Shelf, but there was also dispersal from the Florida Panhandle to the West Florida Shelf. Therefore, the West Florida Shelf may serve as a stepping-stone that facilitates filial connectivity (Legrand et al. 2022) between scamp near the Florida Panhandle and those in the Atlantic. In addition, because there is also dispersal from the Florida Panhandle to Louisiana, there may be coalescent connectivity (Legrand et al. 2022) between scamp in Louisiana and the Atlantic because they share common ancestors (i.e. spawners near the

Florida Panhandle). Thus, under the conceptual framework outlined by Legrand et al. (2022), the connectivity pathways revealed by our simulations could lead to broad spatial mixing among scamp throughout the Gulf of Mexico and the US Atlantic.

The fact that such a large proportion of Atlantic recruitment comes from the Gulf of Mexico, even though our findings generally favor a pattern of local retention, may initially seem incongruous. This phenomenon likely arises, however, because of the way that the oceanographic transport patterns overlay the scamp spawning distribution. One of the most ubiquitous circulation patterns in the Gulf is the presence of the meandering Loop Current, which enters the Gulf flowing northward from the Yucatan Straits, rotates clockwise, flowing eastward and then southwards along the outer West Florida Shelf (Hetland & Hsueh 1999, Le Hénaff & Kourafalou 2016). The dispersal pathway connecting the Gulf and Atlantic scamp populations passes through the Straits of Florida, a relatively narrow channel between Cuba and the Florida Keys. When entering the Florida Straits, the Loop Current originates the eastward flowing Florida Current, which dominates the Straits circulation, along with locally and remotely generated mesoscale eddies also translating eastward (Le Hénaff & Kourafalou 2016). Upon exiting the Florida Straits, the Florida Current joins the Gulf Stream, which flows northeastward. Thus, prevailing current patterns in our study region facilitate the dispersal of potential recruits from the Gulf to the Atlantic, but relatively few simulated larvae were transported upstream in the Florida Straits, from the Atlantic to the Gulf. As a result, larvae transported out of the Gulf of Mexico can find acceptable settlement habitat in the Atlantic, but larvae transported out of the Atlantic within the Gulf Stream are removed from the system entirely. For scamp, this is exacerbated by the relative spawning in the 2 regions. Because scamp biomass is higher in the Gulf of Mexico than in the Atlantic (SEDAR 2022a,b), the amount of spawning is higher as well (Fig. 1B). Therefore, more larvae originate in the Gulf of Mexico than in the Atlantic. When combined with the observed larval dispersal pathways, this distribution leads to a large proportion of potential Atlantic recruits coming from the Gulf of Mexico even though most larvae settled close to their spawning grounds.

This set of conditions may not be geographically widespread, but that does not imply that the findings are limited to scamp. Even if these transport dynamics are unique to this region, the results are likely applicable to an extensive set of reef-associated species that span the Gulf of Mexico and the US South Atlantic. Indeed, results for red snapper suggest that up to one-third of Atlantic recruits come from spawning areas in the Gulf of Mexico (Karnauskas et al. 2022). We expect the extent of Atlantic recruitment from the Gulf of Mexico to be highest for species that spawn on the West Florida Shelf, have higher biomass in the Gulf of Mexico than in the Atlantic, and have extended PLDs. By contrast, the effect may be tempered in species with spawning concentrations farther west in the Gulf of Mexico or species with higher abundance in the Atlantic, such as black sea bass *Centropristis striata*.

This connectivity between the 2 regions has important implications for the assessment and management of economically important species. Currently, scamp and other reef-associated fishes near the southeast US are assessed and managed as 2 distinct stocks: one in the US Gulf of Mexico and one in the Atlantic. For scamp, our results suggest that the 2 stocks are connected through source–sink recruitment dynamics, with some Atlantic recruits originating in the Gulf of Mexico. Considering these findings, resource managers may wish to revisit the hard separation of jurisdictional regions or, if this is not feasible, recognize that management decisions applied in the Gulf of Mexico will likely influence scamp abundance in the Atlantic.

For stock assessment, these results may inform our understanding of the spawner–recruit relationship and how that relationship is modeled. Ideally, the stock assessment could incorporate an index of connectivity as a covariate in the recruitment model. Doing so could help explain variance in annual recruitment patterns (Hidalgo et al. 2019) and improve short-term forecasts if the terminal year of the assessment lags behind the terminal year of the hydrodynamic models.

Precisely estimating annual connectivity dynamics would be helpful for stock assessment, but it was not our goal. Instead, we probabilistically informed the general dispersal patterns of scamp. Specifically, even though we used ocean velocity estimates for different years, all of our simulations used the same seasonal and spatial spawning distributions. Similarly, we assumed the same spatial settlement criteria and PLD for all years. In reality, the spatiotemporal dynamics of spawning and settlement are complex processes influenced by many factors (e.g. temperature, trophic interactions, oceanographic processes). Therefore, they are likely to change from year to year, but we did not have sufficient data to model these spatiotemporal nuances. Future simulations could consider exploring annual variation in both spawning

(e.g. Di Stefano et al. 2023) and settlement (e.g. Druon et al. 2015), particularly if they aim to hindcast recruitment estimates for specific years.

Similarly, our results must also be considered at the appropriate spatial scale. Scamp are thought to form transient spawning aggregations in rocky areas with high local relief (Coleman et al. 2011, SAFMC 2013, Farmer et al. 2017, Grüss et al. 2018, Heyman et al. 2019, Biggs et al. 2021). We included these factors, when possible (e.g. local relief from modeled bathymetry), but fine-scale habitat information is not available throughout our study area and the details of scamp aggregation behavior remain uncertain. Therefore, our spatial models are likely to approximate the broad spatial trends in scamp spawning but they cannot account for fine-scale patterns due to habitat patchiness, local movements, or transient aggregations.

In addition, the spatial resolution of the ocean circulation models in our study area ranged from 2 to 8 km (Table 3), so they cannot resolve flow at finer spatial scales. Consequently, the results of our dispersal simulations can probabilistically inform the general connectivity patterns expected for scamp and help to identify which spawning or settlement regions are likely important. They cannot, however, precisely identify specific spawning or settlement locations or be used to compare neighboring locations with certainty.

To explore whether our results were robust to alternative assumptions of scamp larval biology and ocean circulation, we conducted a suite of sensitivity analyses. The goal of these explorations was not to disentangle the relative importance of physical oceanography and larval biology on the ultimate dispersal patterns of scamp but rather to understand how known uncertainties might influence our findings. Our general conclusions were robust to the choice of hydrodynamic model and assumed larval biology, but there was considerable quantitative variation across the simulation results.

The greatest variation was across simulations in the hydrodynamic ensemble, which used different ocean velocity fields but the same biological parameterization. For example, the simulation that relied on velocity fields from the GOM HYCOM HiRes model estimated that 56% of Atlantic recruits came from the Gulf of Mexico, while the simulation using velocity fields from the SABGOM model estimated that only 19% did (Table 5). This is consistent with results for red snapper (Karnauskas et al. 2022), which also found that SABGOM provided lower estimates of Atlantic recruitment coming from the Gulf of Mexico than other hydrodynamic models. This is most likely due to differences in the hydrodynamic models themselves, as SABGOM presented lower variability than other models (Karnauskas et al. 2022). This variability in the flow field, which is largely due to the formation and passage of mesoscale eddies, is essential to facilitate connectivity between the Gulf and Atlantic regions.

It is hard to completely exclude the possibility of a year effect, however, as we were constrained by the years that ocean velocity estimates were available. Therefore, our SABGOM simulation used an earlier set of years (2003–2010) than the other simulations, which started in or after 2010. This difference in year sets can influence connectivity estimates because of unpredictable changes in the state and position of the Loop Current that lead to considerable year-to-year variability in the circulation patterns in the northeast Gulf of Mexico (Liu et al. 2016). Therefore, the degree to which the Loop Current extends north into the Gulf of Mexico and the seasonal timing of these intrusions are likely to change from one year to the next, which will, in turn, influence the annual estimates of connectivity. However, variability in the Loop Current is greatest on time scales of 2 yr or less (Liu et al. 2016), so because we used at least 5 yr for most hydrodynamic models, the results are probabilistically robust (Karnauskas et al. 2022). Therefore, we can compare the general patterns across simulations, even those that used different years.

In addition, there was still considerable variation between hydrodynamic models that used largely overlapping years (e.g. Mercator, HYCOM, HYCOM-HiRes). Even within a given simulation year, different hydrodynamic models provided different estimates of how many Atlantic recruits came from the Gulf (Table 5). However, it was not simply that one hydrodynamic model consistently provided higher estimates than another and they all followed the same trend from one year to the next. Instead, there were also differences in the interannual patterns between simulations that use different velocity fields (Fig. 5). This variation is likely because the mechanistic factors that control when and how far the Loop Current intrudes into the Gulf of Mexico are not fully understood (Weisberg & Liu 2017, National Academies of Sciences, Engineering, and Medicine 2018).

There was less variation across the simulations in the biological ensemble, which all used the same hydrodynamic model. This does not, however, imply that variability in current velocity estimates is more important in determining dispersal patterns than variability in larval biology. Indeed, biological assumptions, like the vertical distribution of larvae in the water column,

can have profound implications for the ultimate dispersal patterns (Hernández et al. 2023). In our case, the alternative biological assumptions we considered apparently presented smaller variations around the base simulation than the alternative flow representations did. Even still, changing the biological parameterization did influence our simulated recruitment dynamics (Table 4) and connectivity estimates (Table 5, Fig. 5). Relative to the base simulation, increasing the PLD and extending the settlement criteria to 45 m both increased the proportion of potential Atlantic recruits that came from the Gulf of Mexico. Conversely, incorporating ontogenetic vertical migration decreased the proportion of potential Atlantic recruits that spawned in the Gulf. This is largely because of a decrease in the proportion of Gulf of Mexico-spawned larvae that successfully settled, an increase in the proportion of Atlantic-spawned larvae that successfully settled (Table 5), and a corresponding increase in local retention in the Atlantic, particularly near North Carolina (Fig. S12). Not surprisingly, the variation that did exist remained consistent from one year to the next. For example, the simulation using a settlement criterion of 45 m always resulted in the highest estimate of connectivity (Fig. 5).

4.1. Research recommendations

Our findings highlight several avenues for future exploration. As suggested by Swearer et al. (2019), empirical observations could help validate our findings and confirm our assumptions. For example, our simulations estimate that approximately one-third of scamp recruitment to the US Atlantic comes from the Gulf of Mexico. This result could be explored empirically through targeted genetic analysis that explores the natal origin of individual scamp in the Atlantic.

In addition, a suite of empirical sampling could target areas where our models predict high scamp spawning. This would both confirm the predictions of our spatial models, which underlie our dispersal simulations, and help to better understand the spatiotemporal dynamics of scamp spawning. Histological sampling could further inform the location and character of spawning sites as well as whether the seasonality of spawning is consistent throughout the scamp's range. Once spawning locations are identified, tagging studies could help reveal the details of transient aggregation behavior and the extent of seasonal spawning migrations, both of which remain uncertain and are likely important for management (Erisman et al. 2017, Heyman et al. 2019, Biggs et al. 2021).

Future connectivity explorations could then incorporate an updated understanding of the spatiotemporal variability in spawning as more empirical data become available. Additional dispersal simulations would also benefit from a better understanding of scamp larval ecology. The vertical distribution of scamp larvae is not well studied, and these assumptions are known to influence the results of dispersal simulations (Hernández et al. 2023). Therefore, additional ichthyoplankton sampling with refined taxonomic classification could better inform future connectivity simulations. Similarly, little is known about scamp's PLD or nursery habitat, so we conducted sensitivity analyses to explore the robustness of our results. Empirical studies looking at larval ingress or targeting newly settled young scamp could help inform these assumptions for future dispersal simulations.

We explored the sensitivity of our results to several sources of uncertainty, but future studies investigating connectivity between the Gulf of Mexico and Atlantic could explore others. Specifically, if those larvae that settle in the Atlantic after starting in the Gulf of Mexico tend to settle later during the PLD than other settlers, then including larval mortality could influence the degree of connectivity between the 2 regions. Finally, diverse fish larvae are known to use a variety of environmental cues to orient their swimming (Faillettaz et al. 2015, Cresci et al. 2019, Leis et al. 2021, Berenshtein et al. 2022). Future simulations could also investigate how this potential orientation behavior might influence the expected connectivity between the Gulf of Mexico and the US Atlantic.

4.2. Synthesis

Taken together, our findings provide strong evidence that episodic but consistent long-distance larval dispersal facilitates the connectivity of scamp populations on a broad spatial scale. Moreover, due to the pattern of directional oceanographic transport and the spatial differences in abundance, this connectivity leads to the US Atlantic scamp population receiving a high proportion of external potential recruits from the Gulf of Mexico. Although this may increase the resilience of the Atlantic population, it also means that the sustainability of the Atlantic population may rely, in part, on the health of spawning populations in the Gulf of Mexico.

Acknowledgements. This work relied on many data products and we thank the following data providers: Alexandra Bozec, Eric Chassignet, and Mathieu Le Hénaff provided ocean

velocity estimates; Jeremiah Blondeau, Matthew Campbell, Chris Gardner, Ted Switzer, and Kevin Thompson provided visual survey data; Linda Lombardi-Carslon, Tracey Smart, and David Wyanski provided histology data; Trika Gerard and Glenn Zapfe provided larval data; Tim MacDonald provided data on age-0 and age-1 scamp. Finally, we thank Nikolai Klibansky for his insight and for reviewing a draft of the manuscript; Chip Collier, Todd Kellison, and Sue Lowerre-Barbieri for helpful conversations; and 3 anonymous reviewers for invaluable suggestions. The scientific results and conclusions as well as any views and opinions expressed herein are those of the authors and do not necessarily reflect those of any government agency. The contributions by A.C.V. were carried out under the auspices of the Cooperative Institute for Marine and Atmospheric Studies (CIMAS), a cooperative institute of the University of Miami and the National Oceanic and Atmospheric Administration, cooperative agreement no. NA20OAR4320472.

LITERATURE CITED

Abesamis RA, Saenz-Agudelo P, Berumen ML, Bode M and others (2017) Reef-fish larval dispersal patterns validate no-take marine reserve network connectivity that links human communities. Coral Reefs 36:791–801

Adamski KA, Buckel JA, Martin GB, Ahrenholz DW, Hare JA (2012) Fertilization dates, pelagic larval durations, and growth in gag (*Mycteroperca microlepis*) from North Carolina, USA. Bull Mar Sci 88:971–986

Addis DT, Patterson WF III, Dance MA, Ingram GW Jr (2013) Implications of reef fish movement from unreported artificial reed sites in the northern Gulf of Mexico. Fish Res 147:349–358

Almany GR, Hamilton RJ, Bode M, Matawai M and others (2013) Dispersal of grouper larvae drives local resource sharing in a coral reef fishery. Curr Biol 23:626–630

Almany GR, Planes S, Thorrold SR, Berumen ML and others (2017) Larval fish dispersal in a coral-reef seascape. Nat Ecol Evol 1:0148

Antoni L, Saillant E (2017) Spatial connectivity in an adult-sedentary reef fish with extended pelagic larval phase. Mol Ecol 26:4955–4965

Bacheler NM, Ballenger JC (2018) Decadal-scale decline of scamp (*Mycteroperca phenax*) abundance along the southeast United States Atlantic coast. Fish Res 204:74–87

Berenshtein I, Faillettaz R, Irisson JO, Kiflawi M, Siebeck UE, Leis JM, Paris CB (2022) Evidence for a consistent use of external cues by marine fish larvae for orientation. Commun Biol 5:1307

Berry O, England P, Fairclough D, Jackson G, Greenwood J (2012) Microsatellite DNA analysis and hydrodynamic modelling reveal the extent of larval transport and gene flow between management zones in an exploited marine fish (*Glaucosoma herbaicum*). Fish Oceanogr 21:243–254

Biggs CR, Heyman WD, Farmer NA, Kobara S and others (2021) The importance of spawning behavior in understanding the vulnerability of exploited marine fishes in the US Gulf of Mexico. PeerJ 9:e11814

Bonanomi S, Therkildsen NO, Retzel A, Hedholm RB and others (2016) Historical DNA documents long-distance natal homing in marine fish. Mol Ecol 25:2727–2734

Botsford LW, White JW, Coffroth MA, Paris CB and others (2009) Connectivity and resilience of coral reef metapopulations in marine protected areas: matching empirical efforts to predictive needs. Coral Reefs 28:327–337

Bottesch M, Gerlach G, Halback M, Bally A, Kingsford MJ, Mouritsen H (2016) A magnetic compass that might help coral reef fish larvae return to their natal reef. Curr Biol 26:R1247–R1271

Bullock LH, Smith GB (1991) Memoirs of the hourglass cruises: seabasses (Pisces: Serranidae). Florida Marine Research Institute, Department of Natural Resources, St. Petersburg, FL

Buston PM, Jones GP, Planes S, Thorrold SR (2012) Probability of successful larval dispersal declines fivefold over 1 km in a coral reef fish. Proc R Soc B 279:1883–1888

Campbell RA, Gales NJ, Lento GM, Baker CS (2008) Islands in the sea: extreme female natal site fidelity in the Australian sea lion, *Neophoca cinerea*. Biol Lett 4:139–142

Carr MH, Robinson SP, Wahle C, Davis G and others (2017) The central importance of ecological spatial connectivity to effective coastal marine protected areas and to meeting the challenges of climate change in the marine environment. Aquat Conserv 27:6–29

Chassignet EP, Hurlburt HE, Smedstad OM, Halliwell GR and others (2007) The HYCOM (Hybrid Coordinate Ocean Model) data assimilative system. J Mar Syst 65:60–83

Coleman FC, Scanlon KM, Koenig CC (2011) Groupers on the edge: shelf edge spawning habitat in and around marine reserves of the northeastern Gulf of Mexico. Prof Geogr 63:456–474

Colin PL, Koenig CC, Laroche WA (1996) Development from egg to juvenile of the red grouper (*Epinephelus morio*) (Pisces: Serranidae) in the laboratory. In: Arreguín-Sánchez F, Munro JL, Balgos MC, Pauly D (eds) Biology, fisheries and culture of tropical groupers and snappers. International Center for Living Aquatic Resources Management, Manila, p 399–414

Cowen RK, Paris CB, Fortuna JL, Olson DB (2003) The role of long distance dispersal versus local retention in replenishing marine populations. Gulf Caribb Res 14:129–137

Cowen RK, Paris CB, Srinivasan A (2006) Scaling connectivity in marine populations. Science 311:522–527

Cresci A, Paris CB, Foretich MA, Durif SM and others (2019) Atlantic haddock (*Melanogrammus aelefinus*) larvae have a magnetic compass that guides their orientation. iScience 19:1173–1178

D'Aloia CC, Bogdanowicz SM, Francis RK, Majoris JE, Harrison RG, Buston PM (2015) Patterns, causes, and consequences of marine larval dispersal. Proc Natl Acad Sci USA 112:13940–13945

D'Aloia CC, Bogdanowicz SM, Andrés JA, Buston PM (2022) Population assignment tests uncover rare long-distance marine larval dispersal events. Ecology 103:e03559

Di Stefano M, Legrand T, Di Franco A, Nerini D, Rossi V (2023) Insights into the spatio-temporal variability of spawning in a territorial coastal fish by combining observations, modeling and literature review. Fish Oceanogr 32:70–90

Druon JN, Fiorentino F, Murenu M, Knittweis L and others (2015) Modelling of European hake nurseries in the Mediterranean Sea: an ecological niche approach. Prog Oceanogr 130:188–204

Dubois M, Rossi V, Ser-Giacomi E, Arnaud-Haond S, López C, Hernández-García E (2016) Linking basin-scale connectivity, oceanography and population dynamics for the conservation and management of marine ecosystems. Glob Ecol Biogeogr 25:503–515

Erisman B, Heyman W, Kobara S, Ezer T, Pittman S, Aburto-Oropeza O, Nemeth RS (2017) Fish spawning aggregations: where well-placed management actions can yield big benefits for fisheries and conservation. Fish Fish 18: 128–144

Faillettaz R, Blandin A, Paris SB, Koubbi P, Irisson JO (2015)

Sun-compass orientation in Mediterranean fish larvae. PLOS ONE 10:e0135213
Faillettaz R, Paris CB, Irisson J (2018) Larval fish swimming behavior alters dispersal patterns from marine protected areas in the north-western Mediterranean Sea. Front Mar Sci 5:97
Farmer NA, Heyman WD, Karnauskas M, Kobara S and others (2017) Timing and locations of reef fish spawning off the southeastern United States. PLOS ONE 12:e0172968
Fitzhugh GR, Koenig CC, Coleman FC, Grimes CB, Sturges WS III (2005) Spatial and temporal patterns in fertilization and settlement of young gag (*Mycteroperca microlepis*) along the West Florida Shelf. Bull Mar Sci 77:377–396
Gardner MJ, Chaplin JA, Potter IC, Fairclough DV (2015) Pelagic early life stages promote connectivity in the demersal labrid *Choerodon rubescens*. J Exp Mar Biol Ecol 472:142–150
Gerlach G, Atema J, Kingsford MJ, Black KP, Miller-Sims V (2007) Smelling home can prevent dispersal of reef fish larvae. Proc Natl Acad Sci USA 104:858–863
Gilmore RG, Jones RS (1992) Color variation and associated behavior in the epinepheline groupers, *Mycteroperca microlepis* (Goode and Bean) and *M. phenax* Jordan and Swain. Bull Mar Sci 51:83–103
Grüss A, Biggs CR, Heyman WD, Erisman B (2018) Prioritizing monitoring and conservation efforts for fish spawning aggregations in the US Gulf of Mexico. Sci Rep 8:8473
Harris PJ, Wyanski DM, Byron White D, Moore JL (2002) Age, growth, and reproduction of scamp, *Mycteroperca phenax*, in the southwestern north Atlantic, 1979–1997. Bull Mar Sci 70:113–132
Hernández CM, Paris CB, Vaz AC, Jones BT and others (2023) Diverse patterns of larval coral reef fish vertical distribution and consequences for dispersal and connectivity. Coral Reefs 42:453–465
Hetland RD, Hsueh Y (1999) A loop current-induced jet along the edge of the West Florida Shelf. Geophys Res Lett 26:2239–2242
Heyman WD, Grüss A, Biggs CR, Kobara S and others (2019) Cooperative monitoring, assessment, and management of fish spawning aggregations and associated fisheries in the US Gulf of Mexico. Mar Policy 109:103689
Hidalgo M, Rossi V, Monroy P, Ser-Giacomi E and others (2019) Accounting for ocean connectivity and hydroclimate in fish recruitment fluctuations within transboundary metapopulations. Ecol Appl 29:e01913
Hyun KH, He R (2010) Coastal upwelling in the South Atlantic Bight: a revisit of the 2003 cold event using long term observations and model hindcast solutions. J Mar Syst 83:1–13
Jones GP, Milicich MJ, Emslie MJ, Lunow C (1999) Self-recruitment in a coral reef fish population. Nature 402: 802–804
Jones GP, Planes S, Thorrold SR (2005) Coral reef fish settle close to home. Curr Biol 15:1314–1318
Karnauskas M, Shertzer KW, Paris CB, Farmer NA and others (2022) Source–sink recruitment of red snapper: connectivity between the Gulf of Mexico and Atlantic Ocean. Fish Oceanogr 31:571–586
Keener P, Johnson GD, Stender BW, Brothers EB, Beatty HR (1988) Ingress of postlarval gag, *Mycteroperca microlepis* (Pisces: Serranidae), through a South Carolina barrier island inlet. Bull Mar Sci 42:376–396
Keller J, Herbig J, Acosta A (2020) Fisheries-independent data for scamp (*Mycteroperca phenax*) from reef-fish visual surveys in the Florida Keys and Dry Tortugas, 1999–2018. SEDAR68-DW-06. SEDAR, North Charleston, SC
Kingsford MJ, Leis JM, Shanks A, Lindeman KC, Morgan SG, Pineda J (2002) Sensory environments, larval abilities and local self-recruitment. Bull Mar Sci 70:309–340
Klein JD, Asbury TA, da Silva C, Hull KL and others (2022) Site fidelity and shallow genetic structure in the common smooth-hound shark *Mustelus mustelus* confirmed by tag-recapture and genetic data. J Fish Biol 100:134–149
Le Corre N, Pepin P, Han G, Ma Z, Snelgrove PVR (2019) Assessing connectivity patterns among management units of the Newfoundland and Labrador shrimp population. Fish Oceanogr 28:183–202
Le Corre N, Pepin P, Burmeister A, Walkusz W and others (2020) Larval connectivity of northern shrimp (*Pandalus borealis*) in the Northwest Atlantic. Can J Fish Aquat Sci 77:1332–1347
Le Hénaff M, Kourafalou VH (2016) Mississippi water reaching South Florida reefs under no flood conditions: synthesis of observing and modeling system findings. Ocean Dyn 66:435–459
Legrand T, Chenuil A, Ser-Giacomi E, Arnaud-Haond S, Bierne N, Rossi V (2022) Spatial coalescent connectivity through multi-generational dispersal modeling predicts gene flow across marine phyla. Nat Commun 13:5861
Leis JM, Caselle JE, Bradbury IR, Kristiansen T and others (2013) Does fish larval dispersal differ between high and low latitudes? Proc R Soc B 280:20130327
Lellouche J, Greiner E, Bourdallé-Badie R, Garric G and others (2021) The Copernicus global 1/12° oceanic and sea ice GLORYS12 reanalysis. Front Earth Sci 9:698876
Lindeman KC, Pugliese R, Welch GT, Ault JS (2000) Developmental patterns within a multispecies reef fishery: management applications for essential fish habitats and protected areas. Bull Mar Sci 66:929–956
Liu Y, Weisberg RH, Vignudelli S, Mitchum GT (2016) Patterns of the loop current system and regions of sea surface height variability in the eastern Gulf of Mexico revealed by the self-organizing maps. J Geophys Res Oceans 121:2347–2366
Lombardi-Carlson LA, Cook M, Lyon H, Barnett B, Bullock L (2012) A description of age, growth, and reproductive life-history traits of scamps from the northern Gulf of Mexico. Mar Coast Fish 4:129–144
Lowe WH, Allendorf FW (2010) What can genetics tell us about population connectivity? Mol Ecol 19:3038–3051
Lowther AD, Harcourt RG, Goldsworthy SD, Stow A (2012) Population structure of adult female Australian sea lions is driven by fine-scale foraging site fidelity. Anim Behav 83:691–701
Marra G, Wood SN (2011) Practical variable selection for generalized additive models. Comput Stat Data Anal 55: 2372–2387
Meylan AB, Bowen BW, Avise JC (1990) A genetic test of the natal homing versus social facilitation models for green turtle migration. Science 248:724–727
Milot E, Weimerskirch H, Bernatchez L (2008) The seabird paradox: dispersal, genetic structure and population dynamics in a highly mobile, but philopatric albatross species. Mol Ecol 17:1658–1673
Montgomery JC, Tolimieri N, Haine OS (2001) Active habitat selection by pre-settlement reef fishes. Fish Fish 2:261–277
National Academies of Sciences, Engineering, and Medicine (2018) Understanding and predicting the Gulf of Mexico loop current: critical gaps and recommendations. National Academies Press, Washington, DC
NOAA National Geophysical Data Center (2023) US Coastal relief model, Vols 2, 3, 4, and 5. https://www.ncei.noaa.gov/products/coastal-relief-model

Okubo A (1971) Oceanic diffusion diagrams. Deep-Sea Res, Oceanogr Abstr 18:789–802
Palumbi SR (2003) Population genetics, demographic connectivity, and the design of marine reserves. Ecol Appl 13:S146–S158
Paris CB, Helgers J, van Sebille E, Srinivasan A (2013) Connectivity modeling system: a probabilistic modeling tool for the multi-scale tracking of biotic and abiotic variability in the ocean. Environ Model Softw 42:47–54
Pearce JM, Blums P, Lindberg MS (2008) Site fidelity is an inconsistent determinant of population structure in the hooded merganser (*Lophodytes cucllatus*): evidence from genetic, mark–recapture, and comparative data. Auk 125:711–722
Punt AE, Butterworth DS, de Moor CL, De Oliveira JAA, Haddon M (2016) Management strategy evaluation: best practices. Fish Fish 17:303–334
R Core Team (2023) R: a language and environment for statistical computing. R Foundation for Statistical Computing, Vienna
Roberts DE, Schlieder RA (1983) Induced sex inversion, maturation, spawning and embryogeny of the protogynous grouper, *Mycteroperca microlepis*. J World Maric Soc 14: 639–649
Rooker JR, Secor DH, DeMetrio G, Schloesser R, Block BA, Neilson JD (2008) Natal homing and connectivity in Atlantic bluefin tuna populations. Science 322:742–744
SAFMC (South Atlantic Fishery Management Council) (2013) Report of the second meeting of the MPA Expert Workgroup. SAFMC, North Charleston, SC
Schobernd CM, Sedberry GR (2009) Shelf-edge and upper-slope reef fish assemblages in the south Atlantic bight: habitat characteristics, spatial variation, and reproductive behavior. Bull Mar Sci 84:67–92
SEDAR (SouthEast Data, Assessment, and Review) (2020) Gulf of Mexico and Atlantic scamp stock ID process final report. SEDAR68-SID-05. SEDAR, North Charleston, SC. https://sedarweb.org/documents/sedar68-sid-05-gulf-of-mexico-and-atlantic-scamp-stock-id-process-final-report/
SEDAR (2022a) SEDAR 68OA — Gulf of Mexico scamp grouper final stock assessment report. SEDAR, North Charleston, SC. https://sedarweb.org/documents/sedar-68-gulf-of-mexico-scamp-final-stock-assessment-report/
SEDAR (2022b) SEDAR 68 — South Atlantic scamp stock assessment report. SEDAR, North Charleston, SC. https://sedarweb.org/documents/sedar-68-atlantic-scamp-final-stock-assessment-report/
Selkoe KA, D'Aloia CC, Crandall ED, Iacchei M and others (2016) A decade of seascape genetics: contributions to basic and applied marine connectivity. Mar Ecol Prog Ser 554:1–19
Smith CL (1971) A revision of the American groupers: *Epinephelus* and allied genera. Bull Am Mus Nat Hist 146: 69–241
Swearer SE, Treml EA, Shima JS (2019) A review of biophysical models of marine larval dispersal. Oceanogr Mar Biol Annu Rev 57:325–356
Teodósio MA, Paris CB, Wolanski E, Morais P (2016) Biophysical processes leading to the ingress of temperate fish larvae into estuarine nursery areas: a review. Estuar Coast Shelf Sci 183:187–202
Thompson KA, Switzer TS, Christman MC, Keenan SF, Gardner C, Overly KE, Campbell M (2020) Indices of abundance for scamp (*Mycteroperca phenax*) using combined data from three independent video surveys. SEDAR68-DW-07, SEDAR, North Charleston, SC
Thorrold SR, Latkoczy C, Swart PK, Jones CM (2001) Natal homing in a marine fish metapopulation. Science 291: 297–299
van Herwerden L, Aspden WJ, Newman SJ, Pegg GG, Briskey L, Sinclair W (2009) A comparison of the population genetics of *Lethrinus miniatus* and *Lutjanus sebae* from the east and west coasts of Australia: evidence for panmixia and isolation. Fish Res 100:148–155
Vaz AC, Karnauskas M, Paris CB, Doerr JC and others (2022) Exploitation drives changes in the population connectivity of queen conch (*Aliger gigas*). Front Mar Sci 9:841027
Vaz AC, Karnauskas M, Smith M, Denson LS, Paris CB, Le Hénaff M, Siegfried K (2023) red snapper connectivity in the Gulf of Mexico. Mar Coast Fish 15:e10275
Weersing K, Toonen RJ (2009) Population genetics, larval dispersal, and connectivity in marine systems. Mar Ecol Prog Ser 393:1–12
Weisberg RH, Liu Y (2017) On the Loop Current penetration into the Gulf of Mexico. J Geophys Res Oceans 122: 9679–9694
Whitney NM, Robbins WD, Schultz JK, Bowen BW, Holland KN (2012) Oceanic dispersal in a sedentary reef shark (*Triaenodon obesus*): genetic evidence for extensive connectivity without a pelagic larval stage. J Biogeogr 39: 1144–1156
Wilson RR, Burns KM (1996) Potential survival of released groupers caught deeper than 40 m based on shipboard and *in-situ* observations, and tag-recapture data. Bull Mar Sci 58:234–247
Wood SN (2011) Fast stable restricted maximum likelihood and marginal likelihood estimation of semiparametric generalized linear models. J R Stat Soc B 73:3–36
Xue Z, Zambon J, Yao Z, Liu Y, He R (2015) An integrated ocean circulation, wave, atmosphere, and marine ecosystem prediction system for the South Atlantic Bight and Gulf of Mexico. J Oper Oceanogr 8:80–91
Young EF, Belchier M, Hauser L, Horsburgh GJ and others (2015) Oceanography and life history predict contrasting genetic population structure in two Antarctic fish species. Evol Appl 8:486–509
Zatcoff MS, Ball AO, Sedberry GR (2004) Population genetic analysis of red grouper, *Epinephelus morio*, and scamp, *Mycteroperca phenax*, from the southeastern US Atlantic and Gulf of Mexico. Mar Biol 144:769–777
Zeng X, Adams A, Roffer M, He R (2019) Potential connectivity among spatially distinct management zones for bonefish (*Albua vulpes*) via larval dispersal. Environ Biol Fishes 102:233–252

Editorial responsibility: Alejandro Gallego, Aberdeen, UK
Reviewed by: W. Heyman and 2 anonymous referees

Submitted: May 22, 2023
Accepted: October 4, 2024
Proofs received from author(s): November 26, 2024